Applied Energy 227 (2018) 180–189

Contents lists available at ScienceDirect

Applied Energy

journal homepage: www.elsevier.com/locate/apenergy

A power dispatch model for a ferrochrome plant heat recovery cogeneration system

Lijun Zhang[a,*], Michael Chennells[a,b], Xiaohua Xia[a]

[a] Department of Electrical, Electronic and Computer Engineering, University of Pretoria, 0002, South Africa
[b] Rustenburg Smelter a Glencore Merafe Venture Operation, South Africa

HIGHLIGHTS

- A power dispatching model is developed for a heat recovery cogeneration system.
- The model maximizes plant owner benefits considering power export to the grid.
- The cogeneration system designed generates both electrical and cooling power.
- Operation of furnaces is modeled to determine the waste heat available for recovery.
- Energy and cost savings obtained are used to evaluate feasibility of the system.

ARTICLE INFO

Keywords:
Waste heat recovery
Organic Rankine Cycle
Economic power dispatching
Optimal power flow

ABSTRACT

A Organic Rankine Cycle waste heat recovery cogeneration system for heat recovery and power generation to relieve grid pressure and save energy cost for a ferrochrome smelting plant is investigated. Through the recovery and utilization of previously wasted heat from the facility's internal smelting process off-gases, the cogeneration system is introduced to generate electrical power to supply the on-site electricity demand and feed electricity back to the utility grid when it is necessary and beneficial to do so. In addition, the cogeneration system generates cooling power through a lithium bromide-water solution absorption refrigeration cycle to meet the cooling requirements of the plant. The heat recovery process for power generation is modeled and the optimal power dispatching between the on-site loads and the utility grid is formulated as an economic power dispatching (EPD) problem, which aims to maximize the plant's economic benefits by means of minimizing the cost of purchasing electricity from the utility and maximizing revenue from selling the generated electricity to the grid. Application of the developed model to a ferrochrome smelting plant in South Africa is presented as a case study. It is found that, for the studied case, more than $1,290,000 annual savings can be obtained as a result of the proposed heat recovery power generation system and the associated EPD model. In addition to this, more than $920,000 annual savings is obtained as a result of the generated cooling power via the proposed absorption refrigeration system. The combined cogeneration system is able to generate up to 4.4 MW electrical power and 11.3 MW cooling power from the recovered thermal energy that was previously wasted.

1. Introduction

The world is in the midst of an energy crisis where a limited energy generation capacity is struggling to keep up with a continuously increasing demand for energy. This is particularly the case in South Africa. It has therefore never been more crucial to look towards and embrace renewable energy resources and new energy technologies to aid in the alleviation of this energy crisis. In conjunction with technology development, the recovery and utilization of waste energy have shown significant potential in the management of this crisis by introducing considerable energy savings [1,2]. One such energy saving opportunity exists in the mining and smelting industry, for example in the ferrochrome (FeCr) industry, in the form of furnace off-gas thermal energy recovery.

It was estimated that around 80% of the world's chromium deposits can be found in the Bushveld Complex in South Africa, which spans an estimated cumulative diameter of almost 300 km [3,4]. Because of the sheer size of the area and the overwhelming deposits of precious metals, such as chromium, in the Complex rock, the mining and smelting of these metals form a vital and influential sector of South Africa's economy [4].

* Corresponding author.
E-mail address: lijun.zhang@up.ac.za (L. Zhang).

http://dx.doi.org/10.1016/j.apenergy.2017.08.019
Received 15 January 2017; Received in revised form 1 August 2017; Accepted 7 August 2017
Available online 12 August 2017

Nomenclature

AD	maximum installed access demand for consumption in MVA
CAC_r	consumption administration charge rate in $/day
COP	coefficient of performance of the cooling system
CRC	consumption reliability charge in $
CRC_r	consumption reliability charge rate in $/kWh
CSC_r	consumption service charge rate in $/day
C_{ph}	specific heat of hot material in kJ/kg·K
DLF	distribution loss factor
E	electrical power generated by the cogeneration system in MW
ERC_r	electricity and rural subsidy charge rate in $/MWh
GAC_r	the generation administration charge rate in $/day
GRC	generation reliability charge in $
GRC_r	generation reliability charge rate in $/kWh
GSC_r	the generation service charge rate in $/day
NAC_r	consumption network access charge rate in $/MVA
NDC_r	network demand charge rate in $/MVA
$P_{i,j}^{load}$	active power consumption of the plant, including consumptions of furnaces and induced draft fans, in MW
Q_h^k	heat transfer of the k-th furnace in kW
$Q_{cool,cold}$	cooling power generated by the cooling system in MW
$Q_{cool,low}$	available low temperature power in MW
$Q_{h,total}$	total extracted heat in MW
$S_{i,j}^{load}$	apparent power consumption of the plant, including consumptions of furnaces and induced draft fans, in MVA
TLF	transmission loss factor
TNC_r	transmission network charge rate in $/MVA
T_{cold}	temperature of hot material outlet from heat exchanger in °C
T_{hot}	temperature of hot material inlet to heat exchanger in °C
$ULVSC_r$	the urban low voltage subsidy charge rate in $/MVA
$\%_{Cr_2O_3,s}$	the mass percentages of the Cr_2O_3 in a dry sample of the ore
$\%_{FeO,s}$	the mass percentages of the FeO in a dry sample of the ore in kg/s
$\%_{H_2O}$	the required moisture percentage in the feed ore to a furnace
η_{ne}	net efficiency of the ORC electricity generation system
gAD	maximum installed access demand for generation in MVA
$gNAC_r$	the generation network access charge rate in $/MVA
m_h^k	hot material mass flow rate of the k-th furnace in kg/s
m_{CO_2}	the mass flow rate of CO_2 extracted from the off-gas of a furnace in kg/s
$m_{Cr_2O_3}$	the mass flow rate of Cr_2O_3 to a furnace in kg/s
m_{FeO}	the mass flow rate of FeO to a furnace in kg/s
m_{N_2}	the mass flow rate of N_2 in the extracted hot material from a furnace in kg/s
m_{O_2}	the mass flow rate of O_2 in the extracted hot material from a furnace in kg/s
m_{ore}	the mass flow rate of the raw material ore to a furnace in kg/s
n	number of furnaces
p_p, p_s, p_o	the price for energy consumed in $/MWh during peak, standard and off-peak periods, respectively
p_p^g, p_s^g, p_o^g	the price for energy sold in $/MWh during peak, standard and off-peak periods, respectively

The smelting of chrome is an energy-intensive production process requiring approximately 3.3–3.8 MWh of electrical energy per ton of FeCr produced [5]. Of the country's 40 GW supply capacity, Ferro-Alloy smelting industries account for almost 5%, a staggering 2 GW of required power.[1] FeCr industries in South Africa have become severely constrained nowadays because of their high energy intensity and the increasing electricity price in the country. As a result, these industries need to seek solutions for more efficient utilization of the limited energy supply, which involves improving operational technologies and processes, and the potential recovery and re-use of wasted energy. Through such improvements, the efficiency of energy utilization can be improved and an overall improvement in the country's economy can be achieved by allowing the FeCr industries to be competitive on a global scale once again.

Various methods and techniques for increasing energy efficiency in the chrome smelting industry have been reported [6–8]. An important topic, the utilization of waste thermal energy for the generation of useful energy, has recently come under scrutiny.

The smelting processes of chrome involve the separation and fusion of materials according to process-specific chemical reactions inside a molten material bath in order to produce FeCr. The chemical processes and reactions require a carbonaceous reductant and extremely high temperatures for the extraction of iron (Fe) and chromium (Cr) metals from the raw feed material, which ultimately fuse to form FeCr [9,5,10].

The two most important furnace internal chemical reactions are therefore the reduction of iron and chromium oxides in the raw material, FeO and Cr_2O_3 respectively, to produce the Fe and Cr. A byproduct of the smelting process and the chemical reactions, along with heat, is carbon monoxide (CO) gas. Because of the open nature of the furnaces and the extremely high temperatures, the CO gas exiting the top of the furnace auto-ignites, using oxygen in the surrounding air to produce carbon dioxide (CO_2). The heat, CO_2 gas and dust particles thrown up from the raw material feed process are extracted from the furnaces and treated at the bagplant section of the facility. Currently, these off-gases are extracted by induced draft fans (ID fans) and passed through trombone coolers, which utilize vast surface areas and ambient temperature to cool the hot material. The cooled off-gasses then flow to the bagplant where they are combined with water and pumped to slimes dams for treatment.

Significant waste of energy occurs in the current cooling process because the thermal energy of the extracted hot material is simply dissipated into the atmosphere. The implementation of a cogeneration system instead of the trombone coolers will allow for the recovery and utilization of the wasted thermal energy for the generation of electricity. In the literature, many applications of waste heat recovery technologies to industrial processes have been published. For example, application of a waste heat recovery system to a company manufacturing large ship and offshore oil-platform chains was reported in [11], with the focus on determining the size of the main cogeneration equipment. A similar study on the recovery of multiple waste heat streams in a refinery was done by [12], in which the procedures for designing the heat recovery network were presented in detail. Only preliminary studies on the application cogeneration systems utilizing furnace off-gasses in FeCr smelting plants have been reported [13]. According to the literature, a waste heat recovery system is most suitable for implementation in a FeCr smelting industry that rejects heat from the furnaces at medium to high temperatures via the off-gas extraction system [14–16]. In addition to electricity generation, an absorption refrigeration cycle can be used to generate cooling power by utilizing the byproduct of the electricity generating system, low-grade thermal energy, which is traditionally directed to the power generation cycle cooling system [17,18]. Therefore, a combined cogeneration

[1] Rodney Jones. Electric Smelting in Southern Africa. http://www.mintek.co.za/Pyromet/Files/2013Jones-ElectricSmelting.pdf.

system is proposed for the recovery and utilization of thermal energy rejected from the smelting process for the generation of additional electrical and cooling energy in this study.

The facilities required for the cogeneration system are widely available today [19,20,17,21]; a waste heat recovery system using Organic Rankine Cycle (ORC) [22–25] as working fluid is identified as the most suitable waste heat recovery system for the specific application. A waste heat recovery cogeneration system from Turboden s.r.l. was considered for electricity generation and a lithium bromide-water solution absorption refrigeration system recommended by Voltas Technologies was adopted as the core equipment for cooling power generation. The interest of this study is, in particular, the optimal operation of this system when applied to FeCr smelting plants. Existing studies on heat recovery cogeneration systems either do not consider the power management of such facilities or only study stand-alone operations of such systems. No study on the operation optimization of such systems in a grid-tied environment has been reported so far. Lack of such operating strategies leads to poor performance of the system in terms of both operating efficiency and financial benefits to the plant owner. This is evidenced by many studies concluding that the proper operation and planning of the equipment and facilities are some of the key factors affecting the effectiveness of systems in both the industrial and residential sectors [26–31]. For instance, energy and associated cost savings were achieved by optimal operation of mining facilities, such as conveyor belts, crushers, coal washing plants and so on [32–40]. Moreover, existing studies on the application of heat recovery cogeneration systems to mineral processing plants, such as [41], are centered around the detailed modeling of the heat recovery efficiency instead of looking into the availability of the thermal energy for recovery and optimal operation of the cogeneration systems.

The heat recovery cogeneration system studied in this paper produces on-site electricity and cooling power supply for the plant and provides support and assistance to the utility grid by feeding the generated energy back into the grid during severely high demand periods. This not only helps the national grid but also enables the mine to obtain savings either through the substitution of electrical energy consumed directly from the utility grid or through the export of the generated electrical energy to the utility grid. Optimal operation of the proposed combined cogeneration system in such a grid-connected environment is a challenging task that depends heavily on the operating status of both the on-site smelting processes and the utility grid. The main function of the operation strategy is similar to the traditional economic power dispatching (EPD) problem [42,36,43–46] and the power flow management problem of hybrid renewable energy systems [47–51]. However, the EPD for the studied cogeneration system is even more challenging. Firstly, unlike the traditional power dispatching for power plants, the power generated by the cogeneration system is not controllable because it is directly affected by the process generating the waste heat. Secondly, the amount of waste heat available from the FeCr smelting plant is difficult to determine because of the chemical reactions involved. Therefore, this study focuses on the development of an EPD algorithm that optimizes the operation of an on-site cogeneration system tied to the national grid in order to maximize the benefits of the plant and help to relieve grid strain by feeding electricity back into the grid during peak demand periods. This will make an already implemented cogeneration system more efficient and help to reach the potential benefits of introducing a new cogeneration system to the plant from the plant owner's perspective. From the utility's point of view, the cogeneration system, together with its optimal operation strategy, helps to deal with peak demand and reducing the its generating costs.

The rest of this study is organized as follows: Section 2 presents the modeling process of the waste thermal energy carried in the furnace off-gas together with the efficiencies of the cogeneration system to determine its potential electricity and cooling power generation capacity. The EPD problem is formulated in Section 3. Section 4 provides a case study based on a real world mine in South Africa, followed by some further discussions on the results achieved in Section 5. Finally, conclusions are given in Section 6.

2. Modeling of the cogeneration system

In order to determine the electrical and cooling power generation capacity of the cogeneration system, the available heat from the internal material smelting process and the efficiencies of the cogeneration system must be determined first. A brief description the FeCr smelting process, the determination of the available waste heat for cogeneration, and modeling of the electrical and cooling power generation systems are given in the following subsections. In particular, the furnace process is modeled from first principles to determine the available heat for recovery. After that, the efficiencies of the electrical and cooling power generation facilities are estimated based on manufacture supplied information. Finally, an EPD model is developed to optimally control the power flows between the cogeneration system, the on-site load, and the utility grid in pursuit of maximizing the plant owners benefits.

2.1. Description of the FeCr smelting process

The FeCr smelting plant studied utilizes three-phase AC submerged-electrode arc furnaces for the smelting of raw materials to form a molten bath. This bath is tapped off from the furnaces at regular intervals throughout the day and separated into waste slag and molten FeCr using a density separator. After the cooling, crushing and treatment processes, the FeCr is stored in a range of rock sizes for dispatch. The product FeCr is used in the manufacture of stainless steel.

The furnaces operate at a temperature around 1500 °C. Hot dust and gas are extracted from the furnaces via extraction vents and stacks, at trend-based temperatures from 250 °C to 600 °C, which are determined by the operating conditions of the furnaces. The hot material is then transferred via the extraction ducts to a bagplant, where it is compressed into a fine powder and mixed with water to produce sludge. This sludge is pumped to slimes dams around the facility for treatment. In the existing system, an intermediate cooling process using trombone coolers is implemented between the furnaces and the bagplant to bring the temperature of the hot materials below the maximum temperature rating of the bags to ensure safety. It is proposed to implement a waste heat recovery cogeneration system, consisting of a heat exchanger for thermal energy recovery and a turbine generator for electricity generation, instead of the trombone coolers to generate electricity from the waste heat, while still performing the required cooling of the extracted hot material.

2.2. Calculation of available recovered heat

The calculation of the total available heat from the furnace off-gases requires the temperatures of the hot materials before and after the proposed heat recovery cogeneration system. The temperatures before and after the trombone coolers are used to determine the available heat per furnace and then combined into total available heat for the cogeneration system. The available heat from each furnace is calculated by:

$$Q_h^k = m_h^k C_{ph}(T_{hot} - T_{cold}), \tag{1}$$

where m_h^k is the sum of the flow rates of CO_2, N_2 and O_2 gasses determined according to the furnace feed receipt and the relevant chemical reactions.

The calculations of m_h^k begin with the calculation of the actual mass flow rates of FeO and Cr_2O_3 in the raw feed material by

$$m_{FeO} = \%_{FeO,s} m_{ore}(1 - \%_{H_2O}), \tag{2}$$

$$m_{Cr_2O_3} = \%_{Cr_2O_3,s} m_{ore}(1 - \%_{H_2O}). \tag{3}$$

Thereafter, the constitution of the off-gas is then calculated according

to the following chemical reactions:

$$FeO + C = Fe + CO, \quad (4)$$

$$Cr_2O_3 + 3\,C = 2Cr + 3CO, \quad (5)$$

$$2CO + O_2 = 2CO_2. \quad (6)$$

Using Eqs. (4)–(6), the mass flow rate of CO_2, m_{CO_2}, in the hot material can be obtained. The total mass flow rate of hot materials m_h^k is then obtained by

$$m_h^k = m_{CO_2} + m_{N_2} + m_{O_2}$$

considering the excess air flows, consisting of N_2 and O_2 gases, caused by the operation of ID fans.

To account for the operational status of the system, such as the furnaces being off at certain time intervals for maintenance, potential faults in the temperature sensors and the minimum temperature required for the recovery of heat via the ORC cogeneration system, two vital assumptions are made to facilitate the estimation of the overall available heat. These assumptions, which apply to each furnace individually, are:

- If the furnace outlet extracted off-gas temperature is below 200 °C at a time instant, the actual furnace itself is assumed to be off, and the overall heat recovery cogeneration system will not consider this specific furnace during this time interval.
- If the measured bagplant inlet off-gas temperature is higher than the measured furnace outlet off-gas temperature, the heat recovery process cannot occur, and the overall heat recovery cogeneration system will once again not consider this specific furnace during this time interval.

In particular, the above assumptions are realized by means of the flow control of ID fans used to extract the off-gasses for each furnace, *i.e.* if a furnace is off, the flow rate of the corresponding ID fan will be set to zero. With the aforementioned assumptions, the overall extracted heat available for cogeneration can be calculated using (7).

$$Q_{h,total} = 0.001 \sum_{k=1}^{n} Q_h^k. \quad (7)$$

2.3. Systems for electrical and cooling power generation

For the specific application, Turboden s.r.l., an Italian leading company in the production and development of ORC heat recovery and turbo generator solutions,[2] was consulted and a specialised heat recovery ORC power generation system was recommended based on the information on the plant shown in Table 1.

The most appropriate working fluid selected by Turboden s.r.l. was Hexamethyldisiloxane. The proposed indirect exchange ORC heat recovery cogeneration system is shown in Fig. 1, in which the thermal energy is transferred from the furnace off-gases to the power generation ORC working fluid via the intermediate heat exchanger which utilizes thermal oil as the heat transfer medium. The ORC working fluid absorbs the heat transferred and is vaporized. The fluid vapor then expands through the turbine which drives an electric generator. The ORC working fluid in the vaporous phase that leaves the turbine passes through the regenerator component, where it is condensed utilizing the condenser and water cooling subsystems. Finally, the working fluid, pre-heated by an internal heat exchanger, cycles back at the required pressure by means of the flow control pressurizing pump and is passed back to the main heat exchanger where the cycle begins again.

Therefore, the power generation cycle in Fig. 1 produces electricity and low temperature heat through the closed thermodynamic cycle that

[2] Turboden s.r.l.: http://www.turboden.eu/en/home.index.php.

Table 1
Customer supplied and assumed system data descriptions.

Data description	Source	Data value	Unit
Thermal energy source	Customer	Smelting off-gases	–
Number of furnaces	Customer	4	–
Total exhaust gas flow rate	Customer	73.5	kg/s
Average exhaust gas temperature	Customer	413	°C
Minimum exhaust gas temperature	Customer	200	°C
Average air temperature (dry bulb)	Assumed	23	°C
Average cooling water temperature (tower water)	Assumed	30	°C
Grid voltage connection for unit	Assumed	Medium voltage	–

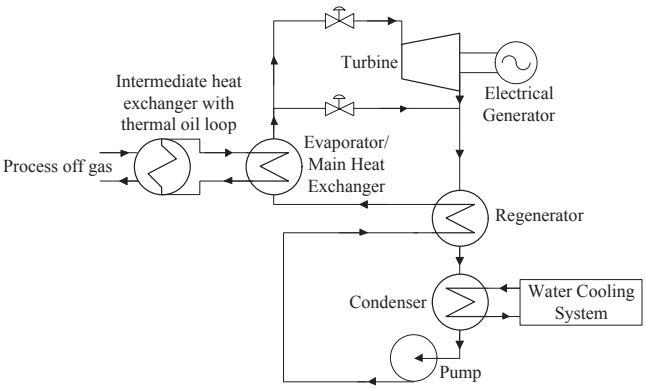

Fig. 1. Turboden s.r.l. indirect exchange ORC heat recovery cogeneration system.

enforces the working fluid to change as defined by the working fluid's characteristic ORC. From the evaluation performed by Turboden s.r.l. utilising the data and descriptions shown in Table 1, the proposed system and performance calculations are shown in Table 2. The net electricity produced by the Rurboden TD40 ORC unit is obtained by

$$E = \eta_{ne} Q_{h,total}, \quad (8)$$

where η_{ne} = net electrical output power/net available thermal power × 100% = 23% for the specific unit.

Traditionally, the low-temperature heat from the ORC cogeneration system is dissipated into the atmosphere via the cooling subsystem. The utilization of the absorption refrigeration cycle allows for the use of this low-grade heat for cooling and refrigeration applications, thereby further improving the overall system energy utilization efficiency. The amount of low-temperature thermal power available, 12.78 MW in the system design case (shown in Table 2), is calculated using

$$Q_{cool,low} = (100\% - \eta_{ne} - 2\%) Q_{h,total}. \quad (9)$$

The low-temperature thermal power calculated in (9) is in the form of hot water. This is because it is the water in the cooling subsystem that picks up the low-grade heat from the power generation cycle via the condenser component. For the suitable operation of an absorption refrigeration cycle, the cooling system fuel or supply heat must be in the form of hot water around 92 °C. Although the proposed power generation system usually operates with condenser design inlet and outlet cooling water temperatures of 23 °C and 30 °C respectively, these design values can be altered with a relatively small reduction in the net efficiency of the electricity generating cogeneration system (about a 2%) in order to obtain a condenser cooling water outlet at approximately 90 °C. Therefore it is assumed that the cooling water exiting the condenser of the power generation system, hot water at approximately 92 °C, will be an acceptable fuel source for the absorption refrigeration system. The utilization of this low-grade thermal energy results in a net efficiency decrease of 2% for the electrical power-generating unit.

A lithium bromide-water solution absorption refrigeration cycle

Table 2
Turboden s.r.l. system and calculated performance characteristics.

Data description	Source	Data value	Unit
Heat source calculations			
Output temperature from exchanger	Turboden	200	°C
Exhaust gas average specific heat capacity	Turboden	1.1	kJ/kg.K
Heat losses from heat exchanger	Turboden	2	%
Net available thermal power	Calculated	17,060	kW
ORC power generation unit			
ORC unit type	Turboden	TD40	–
Heat exchange configuration	Turboden	Indirect exchange	–
ORC gross power output at generator terminals	Calculated	4130	kW
ORC captive power consumption	Calculated	195	kW
ORC net output power	Calculated	3935	kW
Thermal power to cooling source	Calculated	12,700	kW
Electrical generator			
Generator type	Turboden	Asynchronous	–
Generator frequency	Turboden	50	Hz
Generator voltage	Turboden	Medium voltage	–
Cooling subsystem (if required)			
Cooling type (ORC condenser)	Turboden	Dry WCC	–
Cooling system internal consumption	Calculated	180	kW

recommended by Voltas Technologies is chosen for the cooling power generation. Fig. 2 shows the diagram of this cooling power generating unit. The coefficient of performance (COP) of this cooling system is 0.7. Therefore Eq. (10) is used to calculate the cooling power output.

$$Q_{cool,cold} = COP \times Q_{cool,low} = 0.7Q_{cool,low}. \tag{10}$$

The equations from (1)–(10) will be used to determine the available heat from the smelting process, the generated cooling power, and the generated electrical power, which is then used by the EPD algorithm to develop the optimal power dispatch schedule in the following section.

3. EPD model development

The cogeneration system and the energy flow diagram is shown in Fig. 3. As mentioned earlier, the EPD model determines the optimal dispatching of the generated electricity, E, between the on-site loads and the utility grid so that the maximum possible overall savings can be obtained.

The decision variable of the EPD problem is thus the amount of generated electricity, denoted by $C_{i,j}$ in MW, that is dispatched back to the furnace loads. In $C_{i,j}$,$i = 1,2,...,m$ is the index of days in a month and $j = 1,2,...,48$ is the index of hours in a day. To account for the maximum demand charge cost of the plant, which is determined by the recorded maximum power drawn by the plant in a month, the EPD problem is formulated over the period of a month. The sampling period of the EPD problem is taken as half an hour, which is the integrating period of the utility for energy and demand charges, to ease calculations of the overall cost.

The system's overall cost to be minimized is the sum of the system-related energy costs/incentives, use-of-service (UoS) charges and costs, and costs associated with the generation of energy via the cogeneration system. The overall energy cost represents all costs associated with the consumption of energy from the utility grid less the financial incentives obtained through the sell-back of cogeneration generated power to the utility grid. The UoS charges and costs account for all costs and rebates associated with the power supply from the utility grid, including administration and network reliability costs. Lastly, the power generation costs include all costs that are incurred through the process of generating the additional useful electricity via the cogeneration system. To be specific, the cost of power generation includes two parts. The first part is the captive power consumed by the cogeneration system, which is accounted for by (8). The second part is the energy cost of the operation of the ID fans, which is part of the on-site loads.

The overall objective function of the EPD model is therefore summarised in the following equation:

$$\begin{aligned}\text{Overall Cost} = {} & \text{cost of on-site energy consumption} \\ & -\text{total incentive from sold energy} + \text{UoS charges.}\end{aligned} \tag{11}$$

According to the consumption and generation tariff structures set by the local utility, Eskom, overall energy consumption and generation costs are to be determined according to the time-of-use (TOU) tariff [52,53]:

$$p_j = \begin{cases} p_p, & \text{if } j \in \{15,16,...,20\} \cup \{37,38,...,40\}; \\ p_s, & \text{if } j \in \{13,14\} \cup \{21,22,...,36\} \cup \{41,42,43,44\}; \\ p_o, & \text{if } j \in \{1,2,...,12\} \cup \{45,46,47,48\}. \end{cases} \tag{12}$$

Therefore the cost function must account for these TOU periods using peak, standard and off-peak TOU period flag variables. The peak, standard and off-peak flag variables take values of either one or zero and are defined by $P_{i,j} = 1$ if $D(i) = 1, j \in \{15,...,20\} \cup \{37,...,40\}$;$S_{i,j} = 1$ if $D(i) = 1, j \in \{13,14\} \cup \{21,...,36\} \cup \{41,...,44\}$ or $D(i) = 2, j \in \cup \{15...,24\} \cup \{37...,40\}$; and $O_{i,j} = 1$ if $D(i) = 1, j \in \{1,12\} \cup \{45,...,48\}$ or $D(i) = 2, j \in \cup\{1...,14\} \cup \{25...,36\} \cup \{41,...,48\}$ or $D(i) = 3, j \in \cup \{1...,48\}$ with $D(i)$ defined by

$$D(i) = \begin{cases} 1, & \text{if day } i \text{ is a Weekday;} \\ 2, & \text{if day } i \text{ is a Saturday;} \\ 3, & \text{if day } i \text{ is a Sunday.} \end{cases} \tag{13}$$

With the optimization variables and TOU periods defined, the overall system costs for the plant can be determined. The relevant costs under the MEGAFLEX tariff structure [52,53] are discussed in the following subsections.

3.1. Energy consumption-related costs

3.1.1. Network demand charge

A consumption network demand charge (NDC) for the plant's maximum demand is shown in (14).

$$\begin{aligned} NDC = {} & \max\left[|\boldsymbol{S}_{i,j}^{load}| \times \left(1 - \frac{C_{i,j}}{P_{i,j}^{load}}\right) \times (P_{i,j} + S_{i,j}) \right] \\ & \times NDC_r, \text{ for all } i \text{ and } j \end{aligned} \tag{14}$$

3.1.2. Active energy consumption charges

The peak, standard and off-peak active energy consumption charges, PEC, SEC and OEC, respectively, for the total amount of energy consumed, are shown in (15)–(17).

$$PEC = 0.5p_p \sum_{i=1}^{m} \sum_{j=1}^{48} [(P_{i,j}^{load} - C_{i,j}) \times P_{i,j}] \tag{15}$$

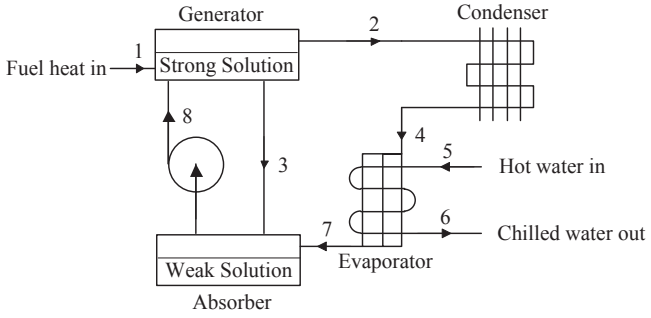

Fig. 2. System incorporated lithium bromide-water solution absorption refrigeration cycle.

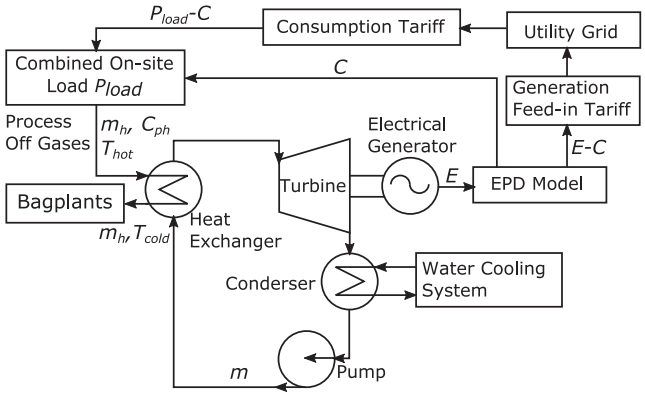

Fig. 3. Waste heat recovery cogeneration system and EPD model energy flow diagram.

$$SEC = 0.5p_s \sum_{i=1}^{m} \sum_{j=1}^{48} [(P_{i,j}^{load} - C_{i,j}) \times S_{i,j}] \quad (16)$$

$$OEC = 0.5p_o \sum_{i=1}^{m} \sum_{j=1}^{48} [(P_{i,j}^{load} - C_{i,j}) \times O_{i,j}] \quad (17)$$

3.1.3. Consumption network related charges

A consumption network access charge (NAC) based on the voltage of power supply and the annual utilised capacity is shown in (18).

$$NAC = AD \times NAC_r \quad (18)$$

A transmission network charge (TNC) is shown in (19).

$$TNC = AD \times TNC_r \quad (19)$$

An urban low voltage subsidy charge (ULVSC) is determined by (20).

$$ULVSC = AD \times ULVSC_r \quad (20)$$

3.1.4. Electrification and rural subsidy charge

An electrification and rural subsidy charge (ERC), applied to the total amount of active energy consumed, is shown in (21).

$$ERC = 0.5ERC_r \sum_{i=1}^{m} \sum_{j=1}^{48} [(P_{i,j}^{load} - C_{i,j}) \times (P_{i,j} + S_{i,j} + O_{i,j})] \quad (21)$$

3.1.5. Reactive energy charge

A reactive energy charge (REC) based on the total amount of excess reactive energy required by the plant is shown in (22).

$$REC = \begin{cases} 0.5REC_r \sum_{i=1}^{n} \sum_{j=1}^{48} [Q_{i,j}^{exc} \times (P_{i,j} + S_{i,j})], & \text{if } Q_{i,j}^{exc} > 0; \\ 0, & \text{otherwise;} \end{cases} \quad (22)$$

where $Q_{i,j}^{exc} = (P_{i,j}^{load} - C_{i,j}) \times \left(\sqrt{\left(\frac{|S_{i,j}^{load}|}{P_{i,j}^{load}} \right)^2 - 1} - 0.3 \right)$.

3.1.6. Consumption service and administration charges

A consumption administration charge (CAC) and a consumption service charge (CSC) for the utilisation of the utility grid are shown in (23) and (24).

$$CAC = m \times CAC_r \quad (23)$$

$$CSC = m \times CSC_r \quad (24)$$

3.2. Energy generation related costs

3.2.1. Generation network access charge

A generation network access charge (gNAC) for the cogeneration system to sell electricity back to the grid is shown in (25).

$$gNAC = gAD \times gNAC_r \quad (25)$$

3.2.2. Active energy generation charges and total rebate

Peak, standard and off-peak active energy generation incentives, PEI, SEI and OEI respectively, for the total amount of active energy sold to or wheeled through the utility grid to third party customers, and a rebate to be subtracted from the *gNAC*, shown in (26)–(29).

$$PEI = 0.5p_p^g \sum_{i=1}^{n} \sum_{j=1}^{48} [(E_{i,j} - C_{i,j}) \times P_{i,j}] \quad (26)$$

$$SEI = 0.5p_s^g \sum_{i=1}^{n} \sum_{j=1}^{48} [(E_{i,j} - C_{i,j}) \times S_{i,j}] \quad (27)$$

$$OEI = 0.5p_o^g \sum_{i=1}^{n} \sum_{j=1}^{48} [(E_{i,j} - C_{i,j}) \times O_{i,j}] \quad (28)$$

$$\text{Rebate} = (PEI + SEI + OEI) \times (DLF \times TLF - 1) \quad (29)$$

The distribution and transmission loss factors, DLF and TLF, in Eq. (29) are given in [52,53]. The rebate is to be subtracted from *gNAC* only if this charge is applicable. If the gNAC is not applicable, the rebate will be 0.

3.2.3. Generation service and administration charges

A generation administration charge (GAC) and a generation service charge (GSC) for the utilisation of the utility grid are shown in (30) and (31).

$$GAC = m \times GAC_r \quad (30)$$

$$GSC = m \times GSC_r \quad (31)$$

3.3. System network reliability service charge

A combined reliability service charge (RSC) based on the supply voltage of the utility grid for both energy consumption and generation is shown in (32)–(34).

$$CRC = 0.5CRC_r \sum_{i=1}^{n} \sum_{j=1}^{48} [(P_{i,j}^{load} - C_{i,j}) \times (P_{i,j} + S_{i,j} + O_{i,j})] \quad (32)$$

$$GRC = 0.5GRC_r \sum_{i=1}^{n} \sum_{j=1}^{48} [E_{i,j} - C_{i,j}) \times (P_{i,j} + S_{i,j} + O_{i,j})] \quad (33)$$

$$RSC = \max(CRC, GRC). \quad (34)$$

3.4. The final cost function

Considering all costs discussed in Sections 3.1–3.3, the final cost function of the EPD problem is re-written as:

$$\begin{aligned} Cost = {} & NDC + (PEC + SEC + OEC) + ERC + REC \\ & + CAC + CSC + TNC + \max(NAC: (gNAC \\ & + \text{Rebate})) + ULVSC - (PEI + SEI + OEI) \\ & + GAC + GSC + RSC. \end{aligned} \quad (35)$$

The EPD optimization problem is eventually formulated as minimizing system associated cost (35) subject to the available heat for cogeneration (7), the efficiencies of the electrical and cooling power generating units detailed in Sections 2.2 and 2.3, and the energy consumption of the plant.

4. Case study and result analysis

4.1. EPD model data requirements

A case study of a chrome smelting plant in South Africa that utilizes four AC submerged electrode arc furnaces is presented. The EPD algorithm utilizes the raw facility and process-related data in order to calculate the energy generation capacity of the proposed cogeneration system. In particular, the raw data required include the real and apparent load powers of all four furnaces and the associated induced draft fans, in MW and MVA respectively, and the extracted off-gas temperatures before and after the cogeneration system. All data were obtained with corresponding date-time stamps (yyyy/mm/dd hh:mm) with a sampling period of half an hour.

The EPD algorithm utilizes a monthly-based cost function and therefore requires an entire month's data for the optimal power dispatch schedule development. However, the EPD model is expected to operate in real-time, generating a current optimal power dispatch schedule for any time interval in a given month. A forecast model based on historical data is developed to facilitate the real-time operation of the EPD model. The forecast model developed predicts the average daily load profile data array using historical data acquired. This forecast data array is then used by the EPD model and updated every 30 min by the most recent measurement.

The main objective of the EPD model is to provide the facility with energy and cost savings. Therefore, the primary and most important result is the overall system associated energy and cost savings from the heat recovery cogeneration system and the associated EPD model. In addition, this study also serves to investigate the overall capacity of the previously wasted thermal energy from the off-gasses and the cooling power capacity that can be additionally generated using the byproduct, low-grade thermal energy, of the waste heat recovery system.

Process and facility-related raw data were obtained for the time period from 2014/08/01 00:00 to 2014/11/12 12:30. The EPD model was tested using a winter and a summer month, August 2014 and October 2014 respectively, to investigate the effect of seasonal variations.

4.2. Potential of the cogeneration system

Fig. 4 shows the combined on-site loads of the plant studied and the corresponding available thermal powers that can be used by the cogeneration system for a winter month (August) and a summer month (October).

Making use of the raw data and the characteristics of the combined cogeneration system, Fig. 5 depicts the average daily profiles of generated electricity and cooling power from the combined cogeneration system for the studied winter and summer months. In addition, Table 3 shows statistics on the profiles in Figs. 4 and 5 and the overall waste thermal energy recovery efficiency of the cogeneration system.

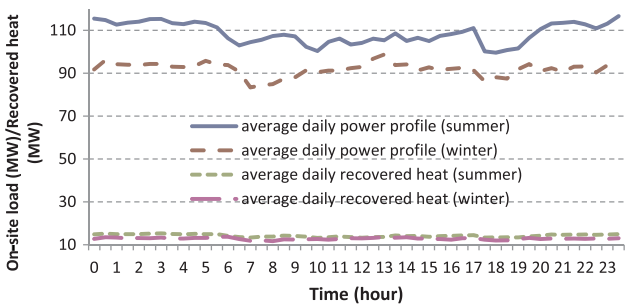

Fig. 4. Average on-site load and recovered heat.

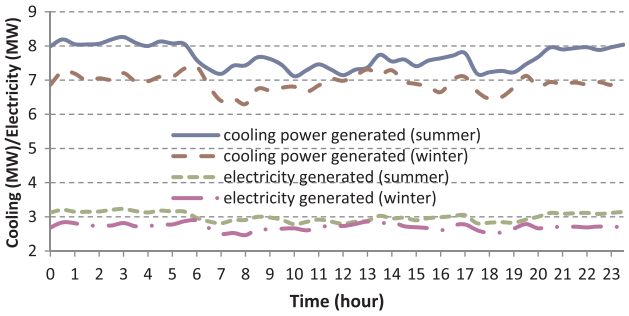

Fig. 5. Average daily generated electricity and cooling power.

4.3. EPD developed optimal power flow schedule

The EPD optimization problem is solved by the *sqp* algorithm built into Matlab. The optimal power dispatch schedule is generated for each half hour interval in the given month. In real-time operation, as time goes by and the following time interval is reached, a new optimal power dispatch schedule is calculated according to the most recent measurement. This process continues until the end of the given month and starts again at the beginning of the following month.

Because of the relatively recent nature of feeding electrical power back to the utility grid in South Africa, no specific feed-in energy tariff structure has been implemented. Currently, a facility feeding electrical power back into the grid obtains a financial incentive from a third-party customer, or Eskom itself, which buys this electrical power. The rates that are implemented for this transaction are the base or wholesale electricity pricing system (WEPS) energy rates. It is noticed that the WEPS energy rates have a significant impact on the EPD model schedule and the overall system associated savings. The WEPS energy rates set by the local utility [52] were found to be too low to allow for or encourage the feed of electrical power back into the utility grid. Consequently, the EPD schedule that was developed dispatched all generated electricity to the on-site loads. For the purpose of this research, the WEPS energy rates are adjusted in order to fully investigate the benefits of the cogeneration system under competitive feed-in tariffs. Table 4 shows the adjusted WEPS energy rates.

The schedules generated by the EPD model for a winter day, 05 August 2014, and a summer day, 10 October 2014, under the adjusted WEPS rates are presented in Figs. 6 and 7, in which different color backgrounds represent the peak (red[3]), standard (yellow) and offpeak (green) periods of the TOU tariff. From these figures, it can be seen that if the WEPS rates encourage this, the EPD would feed the cogeneration generated power back to the grid to support the utility during critical periods.

4.4. System and facility associated savings

To investigate the financial benefits and viability of the proposed cogeneration system, the final system associated cost savings are calculated by subtracting the energy costs of the plant after implementation of the cogeneration system and the associated EPD algorithm from that of the existing system. This is in line with standard protocols on measurement and verification of energy savings (theory and case studies of measurement and verification can be found in [54,55]).

For the chosen winter and summer months the final calculated cost savings obtained are shown in Table 5. Assuming these cost savings are similarly achieved for each winter and summer month respectively, an approximate annual energy cost savings figure of $1351282.80 can be obtained for the plant.

[3] For interpretation of color in Figs. 6 and 7, the reader is referred to the web version of this article.

Table 3
Statistics on the combined averaged daily profiles.

Results	Winter: August 2014			Summer: October 2014		
	Minimum	Average	Maximum	Minimum	Average	Maximum
Average daily load: P_{load} (MW)	84	92.81	100	100	109.5	118
Average daily recovered heat: $Q_{h,total}$ (MW)	11	12.85	14	13	14.26	16
Average daily generated electricity: E (MW)	2.4	2.71	2.9	2.7	3	3.3
Average daily generated cooling power: $Q_{cool,cold}$ (MW)	6.2	6.92	7.4	7.1	7.68	8.3
Average overall waste energy utilization (cooling + electrical) efficiency (%)		74.94			74.89	

4.5. Additional savings from generated cooling power

There are many requirements for cooling throughout the plant, the most prominent being the cooling plant that provides cooling water for the furnace shells. Additional cooling requirements include cooling fans throughout the plant in numerous plant rooms such as the transformer rooms and the hydraulic rooms, office buildings, and so on. The studied plant requires a total facility-wide cooling power of 1.81 MW. The total combined average available cooling power generated via the combined cogeneration system is significantly more than the required cooling capacity of the facility as shown in Section 4.2.

Additional cost savings can be calculated by applying the MEGAFLEX active energy charges to the cooling demand of the plant that is now supplied by the combined cogeneration system. Also, the furnace load can be further reduced because of the reduction in the cooling power required by the furnaces. Utilizing the chosen winter and summer months to calculate additional savings, the overall additional savings are obtained:

- $46742.37 and $30007.80 savings from reduction of the furnace load for August and October 2014, respectively.
- $43658.72 and $45502.95 savings from substituted cooling power for August and October 2014, respectively.

Again assuming these savings are similarly achieved for each summer and winter month, an approximate annual cost savings of $2302082.93 can be obtained for the plant, an increase of $950800.13 due to the utilization of the available cooling power from the proposed absorption refrigeration system.

5. Further discussion of the EPD model results

5.1. Projected payback period

The cogeneration and power generation technologies are still relatively expensive and the success of such a system or project is often determined by its payback period, which is the time it takes for the savings to pay back the capital or project start-up costs. A summary of the potential costs required for the implementation of the proposed combined system is shown in Table 6. Taking into account additional costs for installation and labor, the payback period for the entire system is found to be from 4 to 5 years, which is acceptable for industrial projects.

Table 4
Initial and adjusted WEPS energy rates.

	Peak (c/kWh)	Standard (c/kWh)	Off-Peak (c/kWh)
Adjusted rates for high demand season			
Initial WEPS rates	17.16	5.20	2.82
Adjusted WEPS rates	19.45	6.27	3.61
% Increase	13.39	20.61	28.05
Adjusted rates for low demand season			
Initial WEPS rates	5.60	3.85	2.44
Adjusted WEPS rates	6.69	4.75	3.19
% Increase	19.50	23.43	30.69

5.2. Seasonal variations

The results obtained for winter and summer months are compared with each other to identify the seasonal performance variations. It is found that, although the results do not differ significantly, the comfort cooling required throughout the facility is considerably less in winter. In fact, heating is required rather than cooling in winter. Therefore, an improvement in the system could be made to provide the facility with comfort heating during winter months. In general, it is noticed that slightly more, about 0.18%, cost savings are obtained during winter months. This is because of the much higher active energy consumption rates during winter months, especially during peak and standard TOU periods. Being able to significantly reduce the amount of active energy consumed from the utility grid by the cogeneration system allowed for the slight increase in the overall system associated cost savings during winter months.

5.3. Potential improvements

A number of improvements are identified with regards to this research. The most significant improvements identified are:

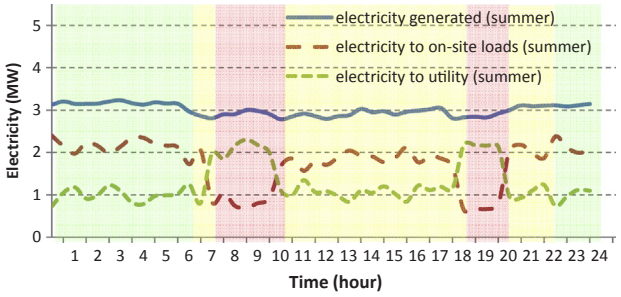

Fig. 6. EPD result of a summer month.

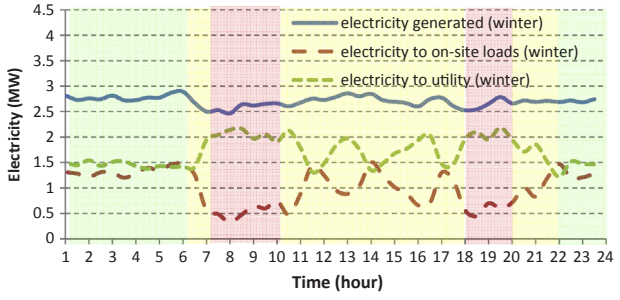

Fig. 7. EPD result of a winter month.

Table 5
Total energy cost and savings.

Parameter	Winter: August 2014	Summer: October 2014
Total initial cost	$5356482.74	$4209939.62
Total final cost	$5215508.85	$4106788.38
Total savings	$140973.88	$103151.24
% Savings	2.63%	2.45%

Table 6
Capital costs associated with the combined cogeneration system.

System component	Cost ($)
Turboden TD40 ORC Unit	4935785.83
Intermediate gas/oil thermal exchanger	3286310.67
2 MW single stage hot water chiller	276578.92
Total cost	8498675.41

- The thermal energy recovery efficiency can be improved by allowing for a lower bagplant inlet temperature.
- The thermal energy recovery efficiency can be improved by convert the open furnaces to closed ones. This will allow for the direct burning of the CO gas in a gas combustion engine, which is much more efficient than the proposed power generation system.
- The excess cooling power, more than 5 MW, can be sold and dispatched to outlying or adjacent facilities to meet additional cooling requirements and to allow for additional financial incentives.

6. Conclusion

Obtaining an optimal operation strategy for cogeneration systems in a grid-connected environment is a challenging task, which has not been well studied in the literature. In this study, the optimal operation of a grid-tied cogeneration system aiming at maximizing the benefits of a ferrochrome smelting plant and aiding the utility grid during peak demand periods is formulated into an optimization problem. The raw material smelting processes and the characteristics of the cogeneration system are modeled first to determine the available process waste heat and the corresponding electrical and cooling power generation capacities of the cogeneration system. The optimization model is designed to make use of the process models and the consumption and feed-in tariffs determined by the utility to dispatch the generated electricity between the on-site loads and the utility grid optimally. The effectiveness of the model is demonstrated by a case study. Further, the optimization model developed can be adapted for similar grid-connected cogeneration systems to improve their efficiency. It can also be used to evaluate the financial viability of new cogeneration projects.

Acknowledgement

The authors would like to thank the reviewers for their insightful comments and suggestions. The quality of this work has been improved significantly because of their inputs.

References

[1] Oluleye G, Jobson M, Smith R, Perry SJ. Evaluating the potential of process sites for waste heat recovery. Appl Energy 2016;161:627–46.
[2] Zhang C, Zhou L, Chhabra P, Garud SS, Aditya K, Romagnoli A, et al. A novel methodology for the design of waste heat recovery network in eco-industrial park using techno-economic analysis and multi-objective optimization. Appl Energy 2016;184:88–102.
[3] Cameron EN. Chromite in the central sector of the eastern Bushveld Complex, South Africa. Am Miner 1977;62:1082–96.
[4] Cawthorn RG. The platinum group element deposits of the Bushveld Complex in South Africa. Platin Met Rev 2010;54(4):205–15.
[5] Pan X. Effect of South African chrome ores on ferrochrome production. In: International conference on mining, mineral processing and metallurgical engineering, Johannesburg, South Africa; 2013.
[6] Roos J, Hearn A. Optimising the effective use of energy in the ferroalloy industry through innovative technology. In: Proceedings of the tenth international ferro alloys congress, Cape Town, South Africa; 2004. p. 712–25.
[7] Ishitobi T, Ichihara K, Homma T. Operational improvements of a submerged arc furnace in kashima works (KF-1) relined in 2006. In: The 12th international ferroalloys congress: sustainable future, Helsinki, Finland; 2010. p. 509–15.
[8] Daavittila J, Honkaniemi M, Jokinen P. The transformation of ferrochromium smelting technologies during the last decades. J South Afr Inst Min Metall 2004;104(9):541–9.
[9] Niemelä P, Kauppi M. Production, characteristics and use of ferrochromium slags. In: 11th International congress on ferroalloys, New Delhi, India; 2007.
[10] Hayes P. Aspects of SAF smelting of ferrochrome. In: 10th International ferroalloys congress, Cape Town, South Africa; 2004.
[11] Sala A, Flores I, Sala J, Millán J, Gómez I, López L. Cogeneration technology for the metal-processing sector. Appl Energy 2008;85(6):516–27.
[12] Yu H, Feng X, Wang Y, Biegler LT, Eason J. A systematic method to customize an efficient organic Rankine cycle (ORC) to recover waste heat in refineries. Appl Energy 2016;179:302–15.
[13] Murray R, de Kock JA. Potential in utilising furnace off-gas at a ferrochrome smelter with gas engines. In: 2015 International conference on the industrial and commercial use of energy, Cape Town, South Africa; 2015. p. 171–7.
[14] Beaty H, Fink D. Standard handbook for electrical engineers. 16th ed. McGraw-Hill Education; 2012.
[15] Dong H, Li J, Li Z, Zhao Y, Cai J. Cogeneration system utilizing waste heat from sinter-cooling process. In: The 2nd international symposium on power electronics for distributed generation systems, Hefei, China; 2010. p. 674–7.
[16] Hung T, Shai T, Wang S. A review of organic Rankine cycles (ORCs) for the recovery of low-grade waste heat. Energy 1997;22(7):661–7.
[17] Sun L, Han W, Jing X, Zheng D, Jin H. A power and cooling cogeneration system using mid/low-temperature heat source. Appl Energy 2013;112:886–97.
[18] Wei D, Lu X, Lu Z, Gu J. Performance analysis and optimization of organic Rankine cycle (ORC) for waste heat recovery. Energy Convers Manage 2007;48(4):1113–9.
[19] Ziviani D, Beyene A, Venturini M. Advances and challenges in ORC systems modeling for low grade thermal energy recovery. Appl Energy 2014;121:79–95.
[20] Liew PY, Lim JS, Alwi SRW, Manan ZA, Varbanov PS, Klemeš JJ. A retrofit framework for total site heat recovery systems. Appl Energy 2014;135:778–90.
[21] Moussawi HA, Fardoun F, Louahlia H. Selection based on differences between cogeneration and trigeneration in various prime mover technologies. Renew Sustain Energy Rev 2017;74:491–511.
[22] Saleh B, Koglbauer G, Wendland M, Fischer J. Working fluids for low-temperature organic Rankine cycles. Energy 2007;32(7):1210–21.
[23] Chen H, Goswami DY, Stefanakos EK. A review of thermodynamic cycles and working fluids for the conversion of low-grade heat. Renew Sustain Energy Rev 2010;14(9):3059–67.
[24] Lecompte S, Huisseune H, van den Broek M, Vanslambrouck B, Paepe MD. Review of organic rankine cycle (ORC) architectures for waste heat recovery. Renew Sustain Energy Rev 2015;47:448–61.
[25] Chen H, Goswami DY, Rahman MM, Stefanakos EK. A supercritical rankine cycle using zeotropic mixture working fluids for the conversion of low-grade heat into power. Energy 2011;36(1):549–55.
[26] Xia X, Zhang J. Energy efficiency and control systems – from a POET perspective. IFAC Proc Vol 2010;43(1):255–60.
[27] Zhuan X, Xia X. Optimal operation scheduling of a pumping station with multiple pumps. Appl Energy 2013;104:250–7.
[28] Wang B, Xia X, Zhang J. A multi-objective optimization model for the life-cycle cost analysis and retrofitting planning of buildings. Energy Build 2014;77:227–35.
[29] Setlhaolo D, Xia X. Optimal scheduling of household appliances with a battery storage system and coordination. Energy Build 2015;94:61–70.
[30] Wu Z, Xia X, Wang B. Improving building energy efficiency by multiobjective neighborhood field optimization. Energy Build 2015;87:45–56.
[31] Ekpenyong UE, Zhang J, Xia X. An improved robust model for generator maintenance scheduling. Electr Power Syst Res 2012;92:29–36.
[32] Zhang S, Xia X. A new energy calculation model of belt conveyor. In: AFRICON, Nairobi, Kenya; 2009.
[33] Xia X, Zhang L. Industrial energy systems in view of energy efficiency and operation control. Annu Rev Control 2016;42:299–308.
[34] Zhang L, Xia X. Control of industrial systems: mining industry as a case study. Control Eng China 2016;23(12).
[35] Xia X, Zhang J. Operation efficiency optimisation modelling and application of model predictive control. IEEE/CAA J Autom Sinica 2015;2(2):166–72.
[36] Elaiw AM, Xia X, Shehata AM. Hybrid DE-SQP and hybrid PSO-SQP methods for solving dynamic economic emission dispatch problem with valve-point effects. Electr Power Syst Res 2013;103:192–200.
[37] Zhang S, Xia X. Optimal control of operation efficiency of belt conveyor systems. Appl Energy 2010;87(6):1929–37.
[38] Zhang L, Xia X, Zhang J. Improving energy efficiency of cyclone circuits in coal beneficiation plants by pump-storage systems. Appl Energy 2014;119(0):306–13.
[39] Badenhorst W, Zhang J, Xia X. Optimal hoist scheduling of a deep level mine twin rock winder system for demand side management. Electr Power Syst Res 2011;81(5):1088–95.
[40] Mathaba T, Xia X. A parametric energy model for energy management of long belt conveyors. Energies 2015;8(12):12375.
[41] Maruoka N, Akiyama T. Exergy recovery from steelmaking off-gas by latent heat storage for methanol production. Energy 2006;31(10-11):1632–42.

[42] Nwulu N, Xia X. A combined dynamic economic emission dispatch and time of use demand response mathematical modelling framework. J Renew Sustain Energy 2015;7(4).
[43] Xia X, Zhang J, Elaiw A. A model predictive control approach to dynamic economic dispatch problem. In: 2009 IEEE Bucharest PowerTech, Bucharest, Romania; 2009. p. 1–7.
[44] Talaq J, El-Hawary F, El-Hawary M. A summary of environmental/economic dispatch algorithms. IEEE Trans Power Syst 1994;9(3):1508–16.
[45] Xia X, Zhang J, Elaiw A. An application of model predictive control to the dynamic economic dispatch of power generation. Control Eng Pract 2011;19(6):638–48.
[46] Xia X, Elaiw A. Optimal dynamic economic dispatch of generation: a review. Electr Power Syst Res 2010;80(8):975–86.
[47] Wu Z, Tazvinga H, Xia X. Demand side management of photovoltaic-battery hybrid system. Appl Energy 2015:294–304.
[48] Tazvinga H, Zhu B, Xia X. Optimal power flow management for distributed energy resources with batteries. Energy Convers Manage 2015;102:104–10.
[49] Sichilalu S, Tazvinga H, Xia X. Optimal control of a fuel cell/wind/pv/grid hybrid system with thermal heat pump load. Sol Energy 2016;135:59–69.
[50] Zhu B, Tazvinga H, Xia X. Switched model predictive control for energy dispatching of a photovoltaic-diesel-battery hybrid power system. IEEE Trans Control Syst Technol 2015;23(3):1229–36.
[51] Tazvinga H, Zhu B, Xia X. Energy dispatch strategy for a photovoltaic-wind-diesel-battery hybrid power system. Sol Energy 2014;108:412–20.
[52] Eskom. Tariff & charges booklet 2014/15; 2014.
[53] Eskom. generator tariff charges 2014/15; 2014.
[54] Xia X, Zhang J. Mathematical description for the measurement and verification of energy efficiency improvement. Appl Energy 2013;111:247–56.
[55] Xia X, Zhang J, editors. Energy efficiency measurement & verification practices: demystifying M & V through south african case studies. Media in Africa, Pretoria, South Africa; 2012.